

A redundant subspace weighting procedure for clock ensemble

Hai Xu(徐海), Yu Chen(陈煜), Mo-Chi Liu(刘默驰), and Yu-Zhuo Wang(王玉琢)

Citation: Chin. Phys. B, 2024, 33 (**4**): 040601. DOI: 10.1088/1674-1056/ad1b43
Journal homepage: http://cpb.iphy.ac.cn; http://iopscience.iop.org/cpb

What follows is a list of articles you may be interested in

Coherent optical frequency transfer via 972-km fiber link

Xue Deng(邓雪), Xiang Zhang(张翔), Qi Zang(臧琦), Dong-Dong Jiao(焦东东), Dan Wang(王丹), Jie Liu(刘杰), Jing Gao(高静), Guan-Jun Xu (许冠军), Rui-Fang Dong(董瑞芳), Tao Liu(刘涛), and Shou-Gang Zhang(张首刚)

Chin. Phys. B, 2024, 33 (**2**): 020602. DOI: 10.1088/1674-1056/ad0629

Robust free-space optical frequency transfer in time-varying link distances conditions

Zhou Tong(童周), Lei Liu(刘雷), Jia-Liang Wang(王家亮), Qian Cao(操前), Zhi-Cheng Jin(金志成), Kang Ying(应康), Shen-Sheng Han(韩申生), Zheng-Fu Han(韩正甫), and You-Zhen Gui(桂有珍)

Chin. Phys. B, 2024, 33 (**2**): 020601. DOI: 10.1088/1674-1056/ad0718

Sympathetic electromagnetically induced transparency ground state cooling of a $^{40}Ca^{+}$–$^{27}Al^{+}$ pair in an $^{27}Al^{+}$ clock

Chenglong Sun(孙成龙), Kaifeng Cui(崔凯枫), Sijia Chao(晁思嘉), Yuanfei Wei(魏远飞), Jinbo Yuan(袁金波), Jian Cao(曹健), Hualin Shu(舒华林), and Xueren Huang(黄学人)

Chin. Phys. B, 2023, 32 (**5**): 050601. DOI: 10.1088/1674-1056/aca39d

Measurements of Majorana transition frequency shift in caesium atomic fountain clocks

Jun-Ru Shi(施俊如), Xin-Liang Wang(王心亮), Fan Yang(杨帆), Yang Bai(白杨), Yong Guan(管勇), Si-Chen Fan(范思晨), Dan-Dan Liu(刘丹丹), Jun Ruan(阮军), and Shou-Gang Zhang(张首刚)

Chin. Phys. B, 2023, 32 (**4**): 040602. DOI: 10.1088/1674-1056/ac8344

Precise measurement of ^{171}Yb magnetic constants for $^{1}S_0$–$^{3}P_0$ clock transition

Ang Zhang(张昂), Congcong Tian(田聪聪), Qiang Zhu(朱强), Bing Wang(王兵), Dezhi Xiong(熊德智), Zhuanxian Xiong(熊转贤), Lingxiang He(贺凌翔), and Baolong Lyu(吕宝龙)

Chin. Phys. B, 2023, 32 (**2**): 020601. DOI: 10.1088/1674-1056/aca14e

---

A redundant subspace weighting procedure for clock ensemble

Hai Xu(徐海)[1,2,†], Yu Chen(陈煜)[3,†], Mo-Chi Liu(刘默驰)[1], and Yu-Zhuo Wang(王玉琢)[1,2,‡]

[1] *National Institute of Metrology, Beijing* 100029, *China*
[2] *Key Laboratory of State Administration for Market Regulation (Time Frequency and Gravity Primary Standard), Beijing* 100029, *China*
[3] *China National Intellectual Property Administration, Beijing* 100088, *China*

(Received 21 September 2023; revised manuscript received 25 December 2023; accepted manuscript online 5 January 2024)

A redundant-subspace-weighting (RSW)-based approach is proposed to enhance the frequency stability on a time scale of a clock ensemble. In this method, multiple overlapping subspaces are constructed in the clock ensemble, and the weight of each clock in this ensemble is defined by using the spatial covariance matrix. The superimposition average of covariances in different subspaces reduces the correlations between clocks in the same laboratory to some extent. After optimizing the parameters of this weighting procedure, the frequency stabilities of virtual clock ensembles are significantly improved in most cases.

Keywords: weighting method, redundant subspace, clock ensemble, time scale

PACS: 06.30.Ft **DOI:** 10.1088/1674-1056/ad1b43

1. Introduction

Accurate and stable time and frequency standards are required in various fields, including satellite navigation, communication engineering, and geographic information science.[1–3] Ensembles of atomic clocks are widely used to maintain their performances on a time scale.[2,4,5] The ensemble time scale plays a major role in time laboratories because it acts as a robust reference in measurements.[6–8] Usually, the noise characteristics of different atomic clocks are assumed to be independent of each other.[9–11] With the increasing demand for high-precision time services, this assumption should be carefully reconsidered and revised.

It is generally acknowledged that the frequency characteristics of atomic clocks are easily affected by laboratory environmental factors, such as temperature, humidity, and magnetic fields, owing to the presence of electrical and optical devices. Output frequency signals generated in similar environments inevitably contain similar fluctuations. Therefore, certain correlations arise between the atomic clocks in an ensemble, particularly for multiple clocks in the same laboratory.[12–14] The existence of such correlations has led researchers to explore how their effects on time-keeping can be weakened or eliminated.[12–14] An intuitive method is to use a high-performance atomic clock as a reference. The performance of this kind of clock is generally three times (and can be up to 10 times) that of other atomic clocks. However, this solution requires a new atomic clock, resulting in extra high costs. Furthermore, when laboratory clocks are replaced with high-performance atomic clocks, the problem of correlations between clocks still occurs. An alternative solution is to make a remote comparison among three or more time-keeping laboratories by using optical-fiber connection. This approach is also very expensive and the maintaining of optical fiber equipment and signal acquisition technology also causes additional economic burdens. Obviously, a simpler and cheaper method is needed to correct correlations between clock signals.

A covariance matrix intrinsically reflects correlations between measured data, and it is an improved strategy to undermine correlations that elements on off-diagonal line of the covariance matrix are reduced and elements on diagonal are enhanced. In this study, atomic clocks used to produce a clock ensemble time scale are numbered and combined into several overlapping subsets. For each clock subset, a series of subspaces is generated by a sliding overlapped window applied to the clock output signals. The average covariance matrix of the clock subset signals in the window is used as a modified covariance matrix to calculate weights for the clock ensemble time scale. The proposed method reduces the influence of correlations between atomic clocks by using this modified covariance matrix generated by the redundant subspace of the clocks' output signals. There are no external requirements for improving the frequency stability of the clock ensemble time scale.

2. Methods

2.1. Motivation

The weight-and-sum (WAS) method is a simple but powerful technique used to join atomic clocks in a clock ensemble.[5,15] The residuals of these clocks, relative to a reference clock, are directly weighted and summed such that the clock ensemble time scale coming from different clocks is re-

[†]These authors contributed equally to this work.
[‡]Corresponding author. E-mail: wangyzh@nim.ac.cn
© 2024 Chinese Physical Society and IOP Publishing Ltd

inforced with respect to noise. In theory, the frequency stability of the clock ensemble time scale should outperform that of any single atomic clock in the ensemble. The general definition of a WAS for the ensemble time scale is

$$z(t) = \sum_{i=0}^{M-1} w_i(t)_i x_i(t), \tag{1}$$

where $z(t)$ is the output of the clock ensemble time scale, M is the number of clocks, and $w_i(t)$ and $x_i(t)$ are the weight and residual relative to the reference of the i-th clock, respectively. The weights are used to control the suppression of off-axis interference. In matrix form, equation (1) can be written as

$$z(t) = w(t)^{\mathrm{T}} X(t), \tag{2}$$

where $w^{\mathrm{T}} = [w_0(t)\, w_1(t) \cdots w_{M-1}(t)]$, w is a column vector of weights, T represents a transpose, and

$$X(t) = \begin{bmatrix} x_0(t) \\ x_1(t) \\ \vdots \\ x_{M-1}(t) \end{bmatrix}.$$

Given that the residuals are time-dependent random variables, an adaptive weight strategy known as the minimum variance weighting (MVW) approach is used.[5,16] This method involves finding the weight w that minimizes the variance of z(t) in Eq. (2). The variance of the WAS output for the clock ensemble time scale in Eq. (2) can be expressed as

$$E\{|z(t)|^2\} = E\{|w(t)^{\mathrm{T}} X(t)|^2\} = w(t)^{\mathrm{T}} R(t)\, w(t), \tag{3}$$

where $R = E\{X(t)\, X(t)^{\mathrm{T}}\}$ is the spatial covariance matrix. The minimum variance optimization can be formulated as

$$\min w(t)^{\mathrm{T}} R(t)\, w(t), \tag{4}$$

subject to $w^{\mathrm{T}}\alpha = 1$, where α is a unit vector, $\alpha = [1, 1, \ldots, 1]^{\mathrm{T}}$, which represents the distribution of all clocks in the clock ensemble. The solution of Eq. (4) is

$$w(t) = \frac{R(t)^{-1}\alpha}{\alpha^{\mathrm{T}} R(t)^{-1}\alpha}, \tag{5}$$

where $R(t)^{-1}$ is the inverse matrix of $R(t)$. If there are no correlations between the measurements, $R(t)$ is a simple diagonal matrix and the weights are simply given by

$$w_i(t) = \frac{r_{ii}^{-1}(t)}{\sum_{i=0}^{M-1} r_{ii}^{-1}(t)}, \tag{6}$$

where w_i is the weight of the i-th clock and $r_{ii}^{-1}(t)$ is the reciprocal of the i-th clock's variance. In the traditional method, $r_{ii}^{-1}(t)$ is the reciprocal of the i-th clock's Allan deviation instead of the clock's variance in a sample window. However, when the residuals are correlated, this approach is no longer accurate. The correlations can lead to a cancellation of the residuals in the MVW method.[12] In this case, the contribution of the clock ensemble time scale is underestimated. Obviously, $R(t)$ is the key to resolving the correlations. The aim is to modify $R(t)$ to make it more like a diagonal matrix, where the correlations between atomic clocks can be effectively suppressed or eliminated. the details of which are discussed in the following subsection.

2.2. Redundant subspace

Theoretically, the ideal covariance matrix is a positive-definite diagonal matrix, and the most troublesome one is negative values for non-diagonal elements. In the latter case, it is difficult to eliminate the correlations in the covariance matrix. On the one hand, it is easy to understand that the greater the number of clocks, the more likely it is that there are negative terms in the covariance matrix. On the other hand, the correlation between any two clocks is negative, which is inconsistent with actual observations. Therefore, a redundant subspace weighting (RSW) procedure is proposed to use overlapping clock subsets to obtain multiple smaller-sized covariance matrices, thereby reducing the possibility of negative values. Averaging the multiple covariance matrices helps each non-diagonal element converge to a non-negative expected value.

Each clock subset defines a subspace, and each of the overlapping subsets constitutes a series of redundant subspace. The proposed operation for residuals from the clocks, described in Refs. [17,18], is similar to the first step in the WAS approach. The discrete vector is in the form of

$$X[n] = \begin{bmatrix} x_0[n] \\ x_1[n] \\ \vdots \\ x_{M-1}[n] \end{bmatrix}. \tag{7}$$

This estimation can be expressed in a vector form as

$$z(n) = w^{\mathrm{T}}[n] X[n], \tag{8}$$

where $w^{\mathrm{T}}[n] = [w_0[n]\, w_1[n] \cdots w_{M-1}[n]]$. It should be noted that the weights are also time-dependent. In this work, the true covariance matrix is replaced with an estimate of the average form

$$\hat{R}[n] = \frac{1}{N}\sum_{l=1}^{N} X_l[n] X_l^{\mathrm{T}}[n], \tag{9}$$

where N is the number of clock subsets. Each subset represents a subspace of the original residual vector space and $X_l[n]$ is the l-th subset. $X_l[n]$ is given by

$$X_l[n] = \begin{bmatrix} x_l[n] \\ x_{l+1}[n] \\ \vdots \\ x_{l+L-1}[n] \end{bmatrix}, \tag{10}$$

where L denotes the size of a subset.

The residual statistics are time-independent, and temporal samples in a moving overlapped window can be used to calculate covariance based on the ergodic hypothesis:

$$x_l[n] = [x_l[n-K]\cdots x_l[n]\cdots x[n+K]], \tag{11}$$

which means that the window size is $2K+1$ temporal samples for each subspace. Defining $N = M-L+1$, a schematic diagram is shown in Fig. 1. A sliding window is applied to all clocks, and overlapping subsets define a series of redundant subspace. Each subspace is an $L\times Q$ sample matrix that is used to calculate an $L\times L$ covariance matrix.

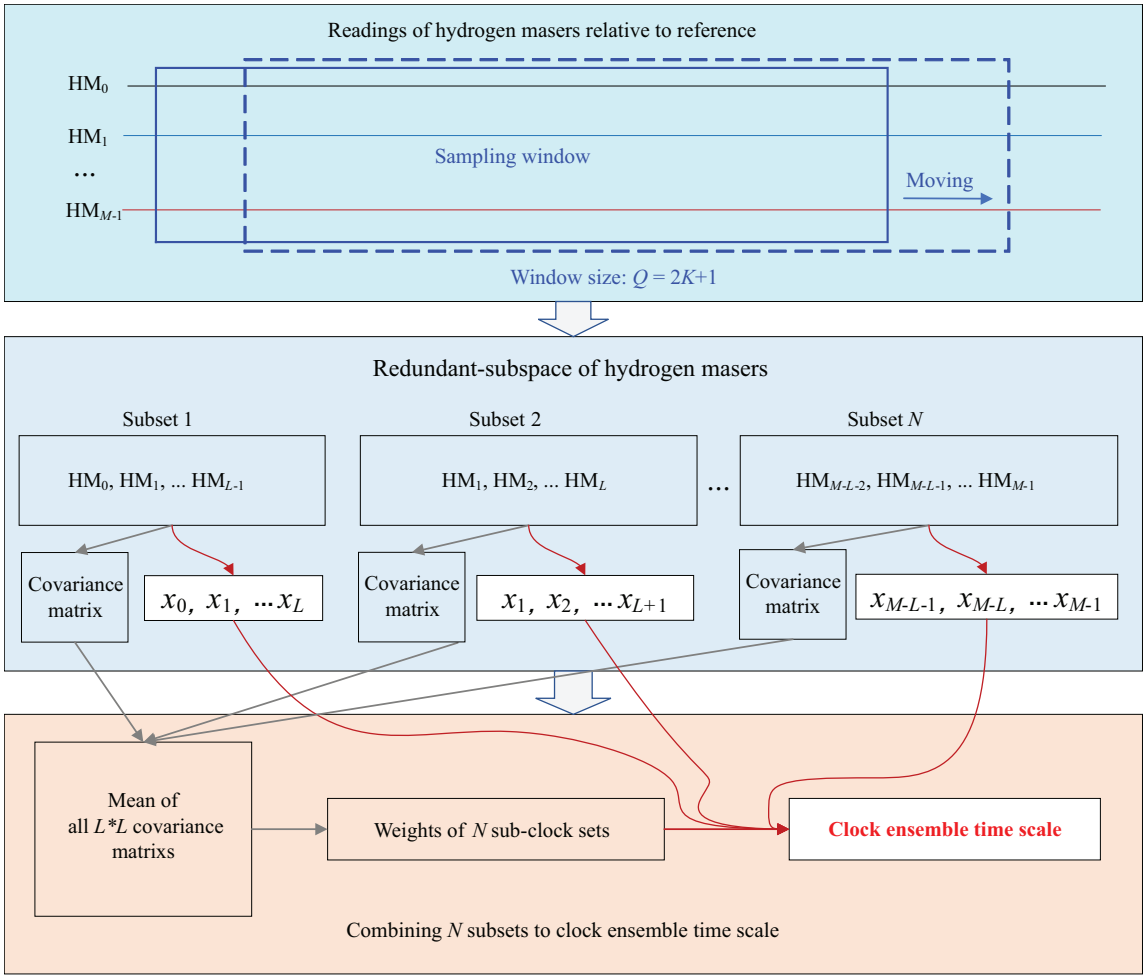


Fig. 1. RSW method outline.

The general estimation of the covariance matrix with all clock subsets is the average of all covariance matrices as follows:

$$\hat{R}[n] = \frac{1}{Q(M-L+1)}\sum_{k=-K}^{K}\sum_{l=0}^{M-L} X_l[n-k]X_l^{\mathrm{T}}[n-k], \tag{12}$$

$$\bar{X}_l[n] = [\bar{x}_l[n]\cdots\bar{x}_{l+L-1}[n]]^{\mathrm{T}}. \tag{13}$$

Here, $\bar{x}_l[n] = x_l[n]$, and using $R[n] = \hat{R}[n]$ in Eq. (2), the estimate for the total set as the average over the subsets is

$$\hat{z}[n] = \frac{1}{M-L+1}\sum_{l=0}^{M-L} w[n]^{\mathrm{T}}\bar{X}_l[n]. \tag{14}$$

It is important to note that although the covariance matrix and $w[n]$ are estimated from residuals indexed as $n-K,\ldots,n+K$, the amplitude estimate depends only on the instantaneous observation of the residual indexed as n.

In addition to overlapping samples used in Eqs. (13) and (14), what is more important is the overlapping atomic clocks and the clock ensemble time scale $\hat{z}[n]$ obtained by weighted average according to $w[n]$. In other words, there are the number of averaging operations in the samples and the number of averaging operations in clocks, and $\hat{R}[n]$ is a semi-positive-definite matrix closer to an approximate diagonal matrix, which can be used to suppress or eliminate the correlations described previously.

2.3. Diagonal loading

An additional parameter can be introduced into Eq. (12) to improve the stability of the calculation, and the associated robust methods belong to the class of diagonal-loading technique. In diagonal loading, a small term is added to the diagonal of the covariance matrix in Eq. (12) before inversion, *i.e.*, $\hat{R}[n]$ is replaced with $\hat{R}[n]+\varepsilon I$, as can be seen by insert-

ing a diagonal matrix into Eq. (12). The $\hat{R}[n]$ then becomes a positive-definite matrix. In many cases, diagonal loading is not necessary because $\hat{R}[n]$ is already a positive-definite matrix. For the stability of the numerical calculation, it is seen empirically that ε in the diagonal loading is proportional to the trace of $\hat{R}[n]$ and given by

$$\varepsilon = \frac{1}{L}\mathrm{tr}\left\{\hat{R}[n]\right\}, \tag{15}$$

where L is the dimension of $\hat{R}[n]$. Consequently, ε is proportional to the average variance of the clock subset residuals.

3. Performance evaluation

Frequency stability is the key objective of a clock ensemble time scale[11,19,20] and is used to evaluate the performances of different weighting methods. To compare the proposed technique with the classic MVW method, simulations were performed following the method described in Ref. [14].

3.1. Simulated clocks

As shown in Ref. [14], the readings from atomic clocks can be modeled as

$$\begin{aligned} x(t) &= x_0 + y\cdot t + \frac{1}{2}d\cdot t^2 + \mu_1\cdot W_1(t) \\ &\quad + \mu_2\cdot\int_0^t W_2(s)\,\mathrm{d}s, \end{aligned} \tag{16}$$

where x and y are the phase time and fractional frequency of the clock, respectively, d represents the frequency drift of the clock, W_1 and W_2 correspond to two independent, one-dimensional standard Wiener processes (standard Brownian motion). The values of W_1 and W_2 can be derived by using

$$\begin{aligned} w_i^1(t) &= w_i^1(0) + N\left(0,{\delta_i^1}^2\cdot t;0,t\right) \quad \text{for } W_i^1, \\ w_i^2(t) &= w_i^2(0) + N\left(0,{\delta_i^2}^2\cdot t;0,t\right) \quad \text{for } W_i^2. \end{aligned}$$

The two terms containing these quantities represent different types of noise. Whereas $\mu_1\cdot W_1(t)$ corresponds to white frequency modulation (WFM) noise, and $\mu_2\cdot\int_0^t W_2(s)\,\mathrm{d}s$ represents random walk frequency modulation (RWFM) noise. The constants μ_1 and μ_2 are diffusion coefficients and provide the intensity of each noise type. The default values of these parameters are listed in Table 1. Here, we ignore the effect of correlations between clocks on clock frequency drift or aging. The fractional frequency, y, of a clock with environmental influence is given by

$$\begin{aligned} y(t) &= \frac{x(t+\tau)-x(t)}{\tau} + S_{\mathrm{ST}}\cdot[T(t)-T(0)] \\ &\quad + S_{\mathrm{DT}}\cdot\frac{\mathrm{d}T(t)}{\mathrm{d}t} + S_M\cdot[M(t)-M(0)] \\ &\quad + S_H\cdot[H(t)-H(0)], \end{aligned} \tag{17}$$

where x is the original phase time of the clock; τ is the time interval, which is set to 1 s; T, M, and H are the temperature, magnetic field, and relative humidity of the ambient environment of the clock, respectively.

Table 1. Typical values of parameters related to Wiener processes, noise, and environmental sensitivities.

Name	Parameter	Typical value
Initial phase time of each clock i	x_0	0
Initial fractional frequency of each clock i	y	1.0×10^{-14}
Frequency drift or aging of each clock i	d	0
"Speed" of the Brownian motion W_i^1	δ_i^1	1
"Speed" of the Brownian motion W_i^2	δ_i^2	3
Diffusion coefficients of frequency modulation noise	μ_1	8.8×10^{-14}
Diffusion coefficients of random walk frequency modulation noise	μ_2	5.6×10^{-18}
Static temperature	S_{ST}	$-5\times10^{-15}/^{\circ}\mathrm{C}$
Dynamic temperature	S_{DT}	$-1\times10^{-14}/(^{\circ}\mathrm{C}\cdot\mathrm{s}^{-1})$
Magnetic field	S_M	$8\times10^{-16}/\mu\mathrm{T}$
Relative humidity	S_H	$2\times10^{-16}/\%$

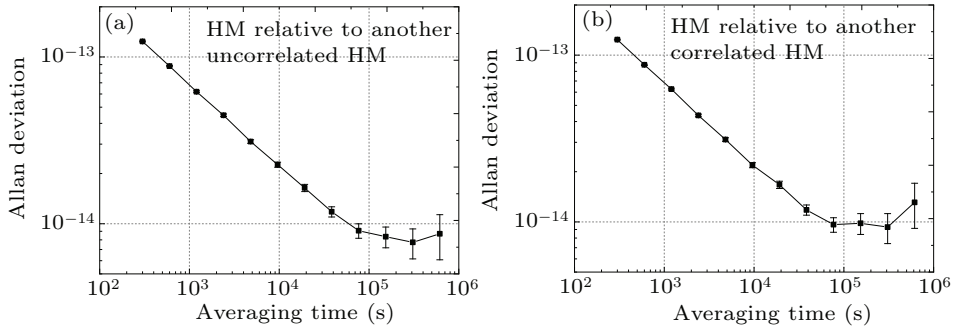


Fig. 2. Frequency stabilities of simulated HMs. (a) Allan deviation of HM relative to another uncorrelated HM (HM-1 relative to HM-20 as a reference). (b) Allan deviation of HM relative to another correlated HM (HM-2 relative to HM-1 as a reference).

Twenty hydrogen masers (HMs) were simulated according to Eq. (16). Then, 10 of these clocks (HM-1 to HM-10; group 1) were further modeled according to Eq. (17), on the assumption that they are in the same environment or have some correlation between them. All the simulation parameters in Eqs. (16) and (17) are listed in Table 1. The remainders of the clocks (HM-11 to HM-20; group 2) were modeled without any environmental parameters and, therefore, were uncorrelated with each other. Here, to match a realistic situation, the simulated data were sampled every 5 min. Figure 2 shows the frequency stability of a simulated clock relative to another HM, expressed by using the Allan deviation. The reference HM was either uncorrelated or correlated to the HM measurement. The rest of the clocks show similar performance because the differences in the simulation parameters were minor.

3.2. Clock ensemble

The proposed technique was applied to three ensembles of the simulated atomic clocks described in the previous subsection. The first ensemble A was relatively small and contained six clocks: three correlated clocks are group 1 and three uncorrelated clocks from group 2. The second ensemble B was intermediate in size and consisted of 10 clocks: five correlated clocks are from group 1 and five uncorrelated clocks from group 2. Finally, the third ensemble C was relatively large and contained 20 clocks: 10 correlated clocks are from group 1 and 10 uncorrelated clocks from group 2. When a subset of clocks was collected, the first clock in the subset was treated as a reference. Therefore, there were two scenarios: one was that the reference was a correlated clock and the other was that it was an uncorrelated clock. Experiments were conducted on all three ensembles for both scenarios and, therefore, on all six possibilities.

In the proposed method, the clocks are divided into subsets, and a sliding window traverses the data in steps and assigns weights to the data for each clock for estimation. Some key parameters, such as the number of subsets and the length and step size of the sliding window, could affect the results. Here, we used a consistent sampling interval of 5 min. Therefore, different combinations of parameter values were tested and tuned to better understand the approach.

3.2.1. Relatively small ensemble of six clocks

Using $\mathrm{HM_{A2}}$ to $\mathrm{HM_{A6}}$ and taking the correlated clock $\mathrm{HM_{A1}}$ as a reference, the classic inverse-variance weighting method is oftensuperior to the proposed technique most of the time (see Fig. 3). However, using $\mathrm{HM_{A1}}$ to $\mathrm{HM_{A5}}$ and taking the uncorrelated clock $\mathrm{HM_{A6}}$ as a reference, the proposed technique with $N = 3$ clock subsets outperforms the MVW method when taking the uncorrelated clock as a reference and when $\tau \geq 3.8 \times 10^4$ s as shown in Fig. 4.

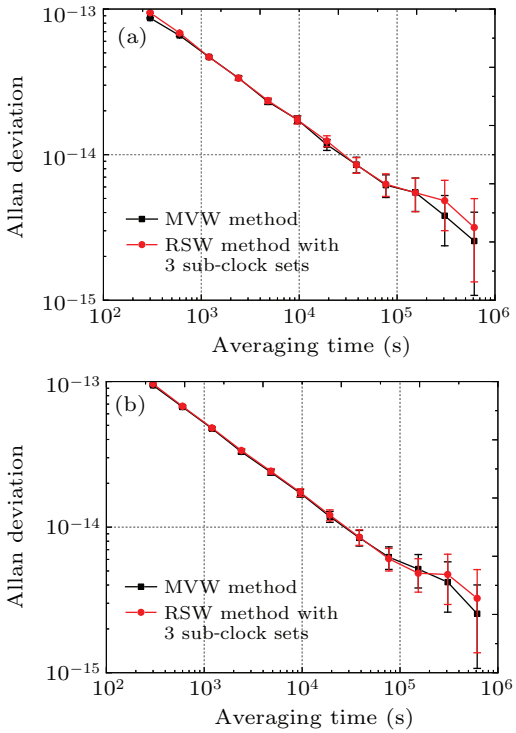


Fig. 3. Allan deviation of weighted $\mathrm{HM_{A2}}$ to $\mathrm{HM_{A6}}$, relative to the correlated reference $\mathrm{HM_{A1}}$, for different lengths of sliding window. RSW with $N = 3$ clock subsets. (a) Window size $Q = 55$ min (11 sample points). (b) Window size $Q = 305$ min (61 sample points).

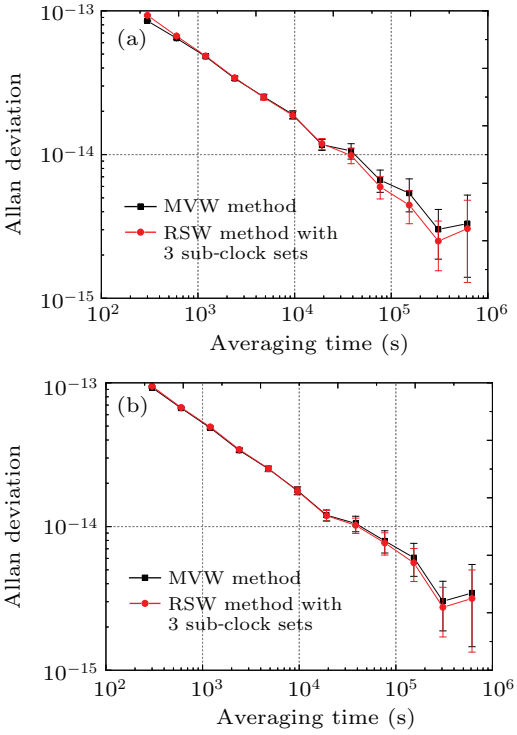


Fig. 4. Allan deviation of weighted $\mathrm{HM_{A1}}$ to $\mathrm{HM_{A5}}$, relative to an uncorrelated reference $\mathrm{HM_{A6}}$, for different lengths of sliding window. RSW with $N = 3$ clock subsets. (a) Window size $Q = 55$ min (11 sample points). (b) Window size $Q = 305$ min (61 sample points).

The average performance improvement for different combinations of window sizes and for different reference groups were calculated and compared. Ten different sets of atomic clocks were randomly and independently generated to calculate the average performance improvement (API), which is

given as follows:

$$\mathrm{API} = \frac{1}{J}\sum_{j=1}^{J}\frac{\mathrm{adev}_{\mathrm{MVW}}(\tau_j) - \mathrm{adev}_{\mathrm{RSW}}(\tau_j)}{\mathrm{adev}_{\mathrm{MVW}}(\tau_j)}, \tag{18}$$

where $\mathrm{adev}_{\mathrm{MVW}}(\tau_j)$ and $\mathrm{adev}_{\mathrm{RSW}}(\tau_j)$ are the Allan deviations of the classic inverse-variance weighted method and the proposed technique, respectively. The improvements for all possible τ values were then averaged and the amount of τ was represented by J. This improvement was calculated for two different window sizes, $Q = 55$ min and $Q = 305$ min.

During several experiments, when the window size Q decreases, there was often a higher average performance improvement and standard deviation of this improvement. The performance improvement was also greater when taking an uncorrelated clock as the reference instead of a correlated clock. When taking a correlated reference clock, the average performance improvement values were -3.71% and -6.01%, respectively, for window sizes of $Q = 55$ min and $Q = 305$ min. Meanwhile, the average performance improvement reached 3.66% and 2.25% for an uncorrelated reference clock for the same window sizes.

3.2.2. Intermediate ensemble of 10 clocks

Figure 5 shows the Allan deviation of 10 weighted HMs. Here we discuss the influence of a different number of clock subsets N on the performance of the method. The proposed technique tends to outperform the MVW method when $\tau \geq 3.8 \times 10^4$ s, with a window size of $Q = 55$ min or $Q = 305$ min for both $N = 7$ and $N = 5$, and when taking an uncorrelated HM as the reference. The average performance improvement is compared for different reference groups, window sizes, and numbers of subsets. The average performance improvement reached 1.86% when $\tau \geq 3.8 \times 10^4$ s.

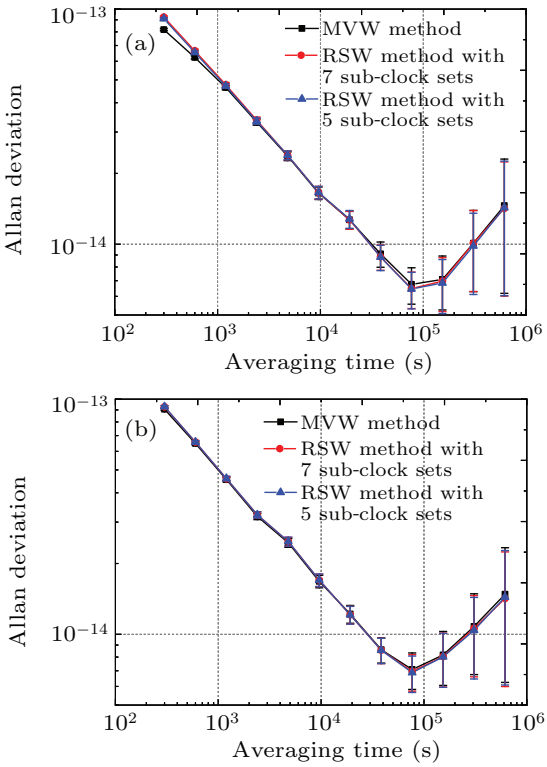


Fig. 5. Allan deviation of weighted $\mathrm{HM}_{\mathrm{B1}}$ to $\mathrm{HM}_{\mathrm{B9}}$ relative to an uncorrelated reference $\mathrm{HM}_{\mathrm{B10}}$ for different lengths of sliding window. RSW with $N = 7$ clock subsets (red line), $N = 5$ subsets (blue line). (a) Window size $Q = 55$ min (11 sample points). (b) Window size $Q = 305$ min (61 sample points).

3.2.3. Relatively large ensemble of 20 clocks

Figure 6 presents the Allan deviations of 20 weighted HMs. The proposed technique outperforms the classic inverse-variance weighted method most of the time when $\tau \geq 3.8 \times 10^4$ s for window sizes $Q = 55$ min and $Q = 305$ min. The average performance improvements are compared for different reference groups, window sizes, and numbers of subsets. When $Q = 55$ min and $N = 10$, the average performance improvement is 1.65%. The performance differences fall within 0.5% for other parameter combinations.

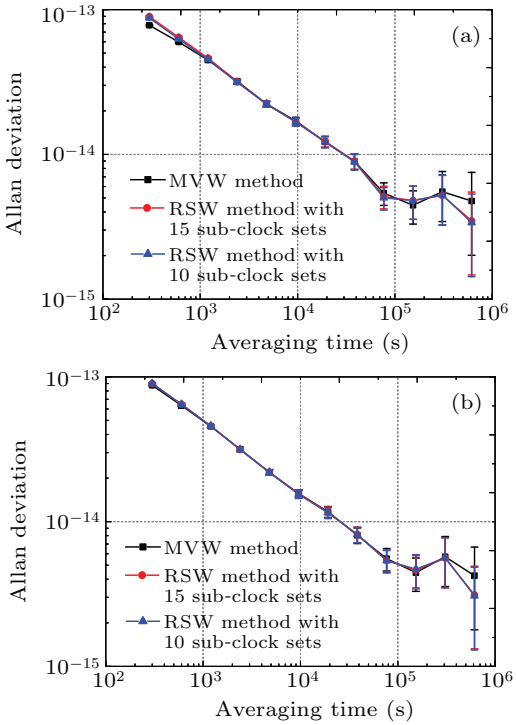


Fig. 6. Allan deviations of weighted $\mathrm{HM}_{\mathrm{C1}}$ to $\mathrm{HM}_{\mathrm{C19}}$ relative to an uncorrelated reference $\mathrm{HM}_{\mathrm{C20}}$ for different lengths of sliding window. RSW with $N = 15$ subsets (red line), $N = 10$ subsets (blue line). (a) Window size $Q = 55$ min (11 sample points). (b) Window size $Q = 305$ min (61 sample points).

From Subsection 3.2.1 to Subsection 3.2.3, it is a certain that the local environment is one of the main reasons affecting the performance of the clock ensemble time scale. Firstly, over a relatively small-time scale (Q chosen from [55 min, 305 min]), the influence of the local environment can be regarded as constant, thereby resulting in an interval correlation between clocks lasting several hours. When time moves to the next period, the local environment itself changed such as the alternation of day and night. In the next period, the clock ensemble time scale also moves to another state, resulting in the

interval correlations for another period. Therefore, Q in each relatively small period is reasonable to eliminate part of the correlations between multiple clocks. On the contrary, if the time interval is large (such as a few days or longer), correlations could become nonlinear and difficult to be represented by the covariance matrix, because the influence of the environment on the clocks themselves will produce a small time or phase shift. Secondly, it can be seen in Figs. 5 and 6 that the stability of the clock ensemble controlled by the RSW method is better than by the MVW method when $\tau \geq 3.8 \times 10^4$ s, and this performance is shown under the condition of different subsets in the clock ensemble. In the case of a large number of subsets, the frequency stabilities for some averaging time have slight fluctuations due to greater uncertainty.

4. Discussion

The above section describes in detail a method of using redundant subspace to address the inaccurate estimation of time scales caused by correlations in atomic clock ensembles. Given the simulated clock residuals, the influences of choosing different combinations of clock subsets, reference clocks, numbers of subsets, and other parameters on the results are now discussed and analyzed.

Overall, when an irrelevant clock is selected as a reference for the time scale, the present technique provides an improvement over the conventional method based on Eq. (6). This advantage could be increased and made more stable with the selection of more suitable values of parameters including the number of clocks, the number of subsets, and the window step size. On the contrary, the details of the relevant clock selected as a reference for the time scale are also shown and compared with MVW in Subsection 3.2.1. Theoretically, such a comparison is meaningless because it could not give actual Allan deviations due to the correlation between the HMs. As proof of concept, the simulation study is to prove that such an operation will not bring any improvement in frequency stability.

Compared with classic MVW method, RSW shows an average performance improvement in frequency stability relative to averaging time that exceeding 10^4 s. Although the RSW herein shows only slight improvement in the simulation clocks' data in long term, it is highly compatible with the correlation according to simulation conditions in Ref. [14].

The limitation of RSW is that the covariance matrix based on simulation clocks' data cannot directly reflect the correlations in short-term due to the fixed conditions (for example, magnetic field parameters, temperature parameters, humidity parameters). As mentioned in Subsection 2.3, ε theoretically is equivalent to adding an extra white noise into the data. For the simulation data, the Allan deviation does not differ by added ε, whose value is always small and substantially unchanged because of the fixed simulated parameters in Table 1. When correlation clocks are used as reference clocks, changes in the clock itself will affect the entire clock group, while when uncorrelation clocks are used as reference clocks, the factors affecting the clock group are usually only related to the environment. And different reference clocks (whether they are correlation clocks or uncorrelation clocks) introduce different noise and have different effects on the results. In addition, the proportion of irrelevant clocks in clock ensemble determines the limitation of RSW performance improvement from theoretical view. If most of the clocks are irrelevant, the correlations among the clocks could be weakened due to the related clocks being rare and their influence on the covariance matrix being negligible. In other words, this does not affect the application of the conventional method to an ensemble with a few relevant clocks. As mentioned above, according to simulation conditions, half the proportion of related clocks in an ensemble may be an acceptable boundary value for using the proposed method. There are no more experiments on simulation data, such as adjusting proportion of related clocks, to demonstrate higher performance improvement of the proposed method, because this is not much meaningful for practical applications.

In the actual usage scenario, all clocks are generally housed in the same environment, which allows them to be related in theory. On the other hand, the physical environment of each laboratory is always different, and there is no reason to think that simulated conditions can be equivalent to specific real environmental conditions. Such differences dictate that correlation between clocks depends on real environmental conditions, which may be manifested in both the long and short term.

The RSW is definitely effective for a clock ensemble with short term correlation. If the correlation between clocks is predominantly manifested in long term, effectiveness of the proposed method depends on the noise introduced by the method itself, the noise brought by correlation, and complexity of real environmental conditions.

5. Conclusions

A technique has been presented to partially eliminate the correlations in an ensemble of atomic clocks and improve the frequency stability of the clock ensemble time scale by using a redundant subspace method. By selecting appropriate parameters of RSW method, it is found that in most cases, the frequency stability can be significantly improved compared with the MVW method. Through the superimposition average of different subspace covariance matrices, the redundant subspace approach is shown to partially reduce the influence of the correlations between atomic clocks induced by the local environment on the frequency stability of the clock ensemble

time scale. Experimental verification is achieved for virtual clock ensembles. The results show that the proposed technique can reduce the frequency instability of the clock ensemble time scale for a certain proportion of related clock sets.

Acknowledgements

Project supported by the National Key Research and Development Program of China (Grant No. 2021YFB3900701), the Science and Technology Plan Project of the State Administration for Market Regulation of China (Grant No. 2023MK178), and the National Natural Science Foundation of China (Grant No. 42227802).

References

[1] Levine J 1999 *Rev. Sci. Instrum.* **70** 062567
[2] Panfilo G and Arias F 2019 *Metrologia* **56** 042001
[3] McGrew W F, Zhang X, Leopardi H, Fasano R J, Nicolodi D, Beloy K, Yao J, Sherman J A, Schäffer S A, Savory J, Brown R C, Römisch S, Oates C W, Parker T E, Fortier T M and Ludlow A D 2018 *Optica* **1811** 05885
[4] Parisi F and Panfilo G 2016 *Metrologia* **53** 1185
[5] Arias E F, Panfilo G and Petit G 2011 *Metrologia* **48** 145
[6] Hachisu H, Petit G, Nakagawa F, Hanado Y and Ido T 2017 *Opt. Express* **25** 8511
[7] Ido T, Hachisu H, Nakagawa F and Hanado Y 2016 *J. Phys.: Conf. Ser.* **723** 012041
[8] Zucca C and Tavella P 2015 *Metrologia* **52** 514
[9] Wang Q, Droz F and Rochat P 2015 *Joint Conference of the IEEE International Frequency Control Symposium & the European Frequency and Time Forum*, Denver, CO, USA, pp. 374–378
[10] Shemar S L, Davis J A and Whibberley P B 2010 *EFTF-2010 24th European Frequency and Time Forum, Noordwijk, Netherlands*, 2010, pp. 1–8
[11] Podogova S and Mishagin K 2014 *European Frequency and Time Forum (EFTF), Neuchatel, Switzerland*, 2014, pp. 568–570
[12] Torcaso F, Ekstrom C R, Burt E A and Matsakis D N 2000 *IEEE Transactions on Ultrasonics, Ferroelectrics, and Frequency Control* **47** 1183
[13] Gao C, Wang B, Zhu X, Li T C and Wang L J 2015 *Joint Conference of the IEEE International Frequency Control Symposium & the European Frequency and Time Forum*, Denver, CO, USA, 2015, pp. 562–564
[14] Guo Y C, Wang B, Si H W, Cai Z W, Zhang A M, Zhu X, Yang J, Feng K M, Han C H, Li T C and Wang L J 2018 *Metrologia* **55** 631
[15] Panfilo G 2009 *IEEE International Frequency Control Symposium Joint with the 22nd European Frequency and Time Forum*, Besancon, France, 2009, pp. xviii–xix
[16] Wang Y Z, Zhang A M, Gao Y, Xu Q H and Lin Y G 2018 *Measurement Science & Technology* **29** 075015
[17] Holm S, Synnevag J F and Austeng A 2009 *IEEE 13rd Digital Signal Processing Workshop and 5th IEEE Signal Processing Education Workshop*, Marco Island, FL, USA, 2009, pp. 60–65
[18] Synnevag J F, Austeng A and Holm S 2007 *IEEE Transactions on Ultrasonics, Ferroelectrics, and Frequency Control* **54** 1606
[19] Zhang A M, Gao Y, Liang K, Wang W B, Yang Z Q, Ning D Y and Fang Z J 2013 *Joint European Frequency and Time Forum & International Frequency Control Symposium (EFTF/IFC)*, Prague, Czech Republic, 2013, pp. 654–657
[20] Sesia I, Cantoni E, Cernigliaro A, Signorile G, Fantino G and Tavella P 2016 *IEEE Transactions on Ultrasonics, Ferroelectrics, and Frequency Control* **63** 575
[21] Zhang A M, Gao Y, Liang K, Yang Z Q, Wang W B, Ning D Y, Zhao K J, Zhang Y, Huang Y, Zhang H and Gao X X 2012 *Journal of Metrology Society of India* **27** 55
[22] Gao Y, Gao X X, Zhang A M, Wang W B, Ning D Y, Wang C, Li D W, Liu X J, Liu N F, Wang P, Li M S, Lin P W, Chen W L, Lin Y G and Li T C 2008 *Metrologia* **45** S34